Solar PV Array Fed Single Stage BLDC Motor Drive for Water Pumping System

Biranchi Narayan Kar[1,*], Paulson Samuel[1],
Jatin Kumar Pradhan[2] and Amit Mallick[2]

[1]*Motilal Nehru National Institute of Technology Allahabad, Prayagraj, Uttar Pradesh, India*
[2]*Veer Surendra Sai University of Technology, Burla, Odisha, India*
E-mail: bnkar@mnnit.ac.in
[*]*Corresponding Author*

Received 27 May 2021; Accepted 25 March 2022;
Publication 24 June 2022

Abstract

A single-stage photovoltaic-fed field-oriented controlled brushless DC (BLDC) motor drive for water pumping using a 2-degree of freedom (DoF) controller is presented in this paper. The proposed 2-DoF controller consists of a feedback and feedforward loop design. A feedback loop is used to maintain stability and desired performance, in which the PI controller is utilized for controlling the DC voltage at the outer loop, which generates the necessary speed reference. A Fuzzy logic controller is then used in the inner loop to achieve a faster speed response of the BLDC motor. Further, the performance of the system is made faster by incorporating dynamic feed-forward control. MATLAB Simulink is used to design and simulate the system. The OPAL-RT simulator is used to validate the system's performance in real-time.

Keywords: Brushless DC motor, fuzzy logic control (FLC), speed control, water pump.

Distributed Generation & Alternative Energy Journal, Vol. 37_5, 1613–1636.
doi: 10.13052/dgaej2156-3306.37513

List of Variables and Abbreviations

Variables:

V_{pv}, I_{pv}, P_{pv}	Voltage (V), Current (A), Power(P) of PV Array
V_{mpp}, I_{mpp}, P_{mpp}	Voltage (V), Current (A), Power(P) of PV Array at maximum power point
V_{oc}, I_{oc}	Voltage (V), Current (A) at open circuit
Vdc	DC Link voltage (V)
P_h	Pump power (kW)
P_m	BLDC motor power (kW)
η_p	Pump efficiency
η_{motor}	Efficiency of BLDC motor
$\eta_{converter}$	Efficiency power converter
C	DC bus capacitor (μF)
ω	Speed of BLDC motor (rad/sec)
N	Speed of BLDC motor (rpm)
K	Proportionality constant
Ic	Capacitor current (A)
I_{inv}	Invertor current (A)
I_d, I_q	Direct axis and quadrature axis current (A)
I_a, I_b, I_c	Three phase stator current (A)
Fsw	Switching frequency (Hz)
K_{pd}	Proportional gain
K_{id}	Integral gain
M	Sampling instant
T_e	Electromagnetic torque (Nm)
N_s, N_p	Number of series and parallel connected module of PV array

Abbreviation:

NB	Negative big
NM	Negative medium
NS	Negative small
PS	Positive small
PM	Positive medium
PB	Positive big

1 Introduction

To meet the electricity demand, renewable energy sources are being promoted by many countries around the globe because of the fast diminishing of conventional energy sources [1, 2]. To generate electricity, renewable energy sources can be used. Solar energy, among many renewable energy sources, is noiseless, pollution-free, and cost-effective, according to [3]. It is cheap and plentiful in the Indian subcontinent and is being applied in numerous applications in addition to water pumping. Photovoltaic-based water pumping for drinking water and irrigation purposes has become highly advantageous for rural areas without grid access. Solar water pumps are more convenient than diesel water pumps for better reliability and lower operational and maintenance expenses.

In a photovoltaic fed water pump system, a DC motor is used in [4] for water pumping. However, due to sparking at the commutator and brush surface, the DC motor is not convenient [5]. In [6] an induction motor is employed for water pumping application fed by a PV array. The induction motor is abundantly used for its low cost, robustness, and reliability. However, high reactive power demand and low efficiency make it inadequate for PV-fed water pumping [7]. Hence, researchers diverged towards a capable and reliable motor for water pumping. The BLDC motor is a good aspirant because of its high power conversion efficiency, high reliability, smooth control, maintenance-free, easy to drive [8–13]. It can certainly compete with induction motors, especially in pumping applications based on photovoltaic arrays, where cost, efficiency, simplicity, and ease of operation are the most critical factors [14]. In addition, the integrated design and motor and pump technologies improve component use and dependability [15].

A PV based water pumping system fed by a double-stage BLDC motor drive was proposed in [16]. The DC-DC converter is utilized for the MPP operation of the photovoltaic array. However, this converter in the intermediate stage affects the efficiency of the system due to size, cost, and complexity. To counteract this issue an attempt has been made to employ a single-stage BLDC motor drive for the water pumping system in [17].

Field-oriented control is mostly used to control the speed of a BLDC motor. A field-oriented controller controls the stator current, epitomized by a space vector. The speed response is improved by separating the three-phase stator current into two-axis, i.e., the d axis and the q axis segments, and controlling them independently [18]. In the field-oriented control method, the speed can be controlled by controlling the quadrature axis current using a PI controller. But due to the fixed gain of the PI controller, it is sensible to parameter variation. Hence, a rule-primarily based controller referred to as a fuzzy logic controller (FLC) is used [19]. FLC creates a set of mathematical models with decision-making based on linguistic principles derived from the designer's previous experience.

To track the maximum power from a photovoltaic array, the MPPT technique is applied between the PV array and the load. Many kinds of literature in the past have used various MPPT techniques to keep the operating point of a photovoltaic array at its maximum powerpoint. Among all the techniques, the perturb and observe MPPT method is the most commonly utilized as it has a low cost and is simple [20]. The disadvantage of this method is that it occasionally deviates from its peak operating point, as in the case of a sudden, ever-changing environmental condition. The MPPT technique, i.e., the incremental conductance (INC) technique, gives outstanding performance for tracking peak power even under changing weather conditions.

In this paper, a water pumping system fed by a PV array with a single-stage BLDC motor drive using a 2-degree of freedom (DoF) controller is presented. An INC technique is utilized for tracking the MPP. A feedback and feed-forward loop design are being used in the proposed 2-DoF controller. To maintain stability and desirable performance, a feedback loop is used, with the PI controller modulating the DC voltage at the outer loop, which generates the required speed reference. In the inner loop, a fuzzy logic controller is being used to achieve a faster speed response of the BLDC motor. Furthermore, the system's performance is improved by implementing dynamic feed-forward control.

2 Structure of the System

The system's structure is depicted in Figure 1. The BLDC-Pump set is powered by a photovoltaic array through a voltage source inverter. The voltage source inverter operates the photovoltaic array at its peak power through appropriate control as well as controls the stator currents.

3 System Design

The system design includes photovoltaic array sizing, the pump, and a BLDC motor so that the operation of water pumping can be executed even at minimum irradiance. The various approaches to the framework are given in the section below.

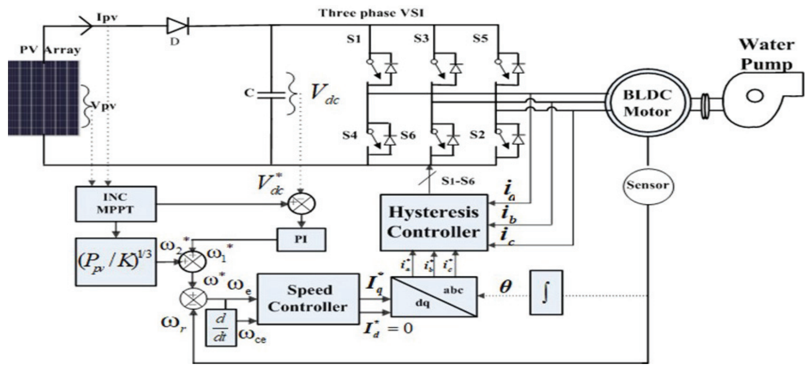

Figure 1 Structure for PV based water pumping system.

3.1 BLDC Motor-Pump Selection

The brushless DC motor and pump are selected mainly based on the volume of water delivery. An assumption has been made in this article that a 14 m^3/h volume of water is to be pumped with 16 m of total dynamic head. Now the pump power is as follows [21]:

$$P_h = \frac{1000 \times 9.8 \times 14 \times 16}{(3.6 \times 10^6)} = 0.6 \text{ kW} \tag{1}$$

Where 1000 kg/m^3 is water density and 9.81m/s^2 is the acceleration due to gravity.

The power of the motor P_m is calculated as

$$P_m = \frac{P_h}{\eta_p} = 0.6/0.6 = 1 \tag{2}$$

Where η_p is the efficiency of the pump which is considered as 60%.

Hence, a 1 kW rated motor is utilized for the application of driving the pump.

3.2 Solar PV Array Sizing

The photovoltaic array's rated power is given by

$$P_{mpp} = \frac{P_m}{(\eta_{motor} \times \eta_{conveter})} = \frac{1}{(0.9 \times 0.95)} = 1.26 \text{ kW} \tag{3}$$

Where η_{motor} and $\eta_{converter}$ are the efficiency of BLDC motor having the efficiency of 90% and converter having the efficiency of 95%.

Hence, a 1.26 kW solar PV array at STC (1000 W/m^2, 25°C) was chosen for the selected BLDC pump. A photovoltaic panel with V_{mpp} and I_{mpp} of 15.44 V and 4.3 A is selected for designing the estimated size of the photovoltaic array.

Here, V_{mpp} for the PV array is chosen as $V_{mpp} = V_{pv} = 300$ V, which is the voltage rating of the motor. The remaining parameters are defined as follows:

$$I_{mpp} = I_{pv} = \frac{P_{mpp}}{V_{mpp}} = \frac{1261}{300} = 4.2 \text{ A} \tag{4}$$

Number of series-connected modules

$$N_s = \frac{V_{mpp}}{V_m} = \frac{300}{15.44} = 19.44 \approx 20 \tag{5}$$

Similarly,

$$N_p = \frac{I_{mpp}}{I_m} = \frac{4.3}{4.2} = 1.02 \approx 1 \tag{6}$$

3.3 Design of Pump

A centrifugal pump combined with a brushless DC motor is chosen for the system. It is designed by utilizing affinity laws of pump that favour torque-speed characteristics as [22, 23]

$$k_1 = \frac{P_m}{\omega^3} = \frac{1000}{(2\Pi \times 3000/60)^3} = 7.14 \times 10^{-5} \tag{7}$$

Where k_1 is the proportionality constant, ω is the speed and P_m is the power of the motor.

With this designed value the pump is adopted for the system.

3.4 Estimation of DC-link Capacitor

The estimation of the capacitor has been done based on ripple current flow to the capacitor and is given by [24, 25]

$$I_c = I_{pv} - I_{inv} \tag{8}$$

where I_{pv} is the current due to solar PV and I_{inv} is the inverter current.

For calculating the ripple current, the worst condition to be considered as I_{inv} is zero.

Hence,

$$I_c = I_{c\ \max} = I_{pv} = 4.3\ \mathrm{A} \tag{9}$$

The capacitor's value is determined by

$$C = \frac{I_{c\max}}{fsw \times \Delta v_{pv}} = \frac{4.3}{10000 \times (19.8 \times 20) \times 0.04} = 63 \approx 100\ \mu\mathrm{F} \tag{10}$$

Where ΔV_{pv} is the photovoltaic voltage ripple, considered to be 4% of the open-circuit voltage (V_{oc}) and *fsw* is the switching frequency.

4 Control Strategy

4.1 Maximum Power Tracking

This method is mainly utilized to track the maximum power of photovoltaic arrays. In this system, an MPPT technique known as an Incremental conductance (INC) is utilized [26, 27]. The instantaneous value of conductance is compared to its incremental value by the INC technique to track MPP [28, 29]. The slope of P-V characteristics is altered based on this value. The operating principle of the INC can be evaluated from the following equation [30]:

$$P_{pv} = V_{pv} \times I_{pv} \tag{11}$$

$$\frac{dP}{dV} = \frac{d(IV)}{dV} = I + V\frac{dI}{dV} = I + V\frac{\Delta I}{\Delta V} \tag{12}$$

At maximum power point,

$$\frac{dP}{dV} = 0 \tag{13}$$

Hence,

$$\frac{\Delta I}{\Delta V} = \frac{-I}{V} \quad \text{at MPP} \tag{14}$$

$$\frac{\Delta I}{\Delta V} > -\frac{I}{V} \quad \text{at the left of MPP} \tag{15}$$

$$\frac{\Delta I}{\Delta V} < -\frac{I}{V} \quad \text{at the right of MPP} \tag{16}$$

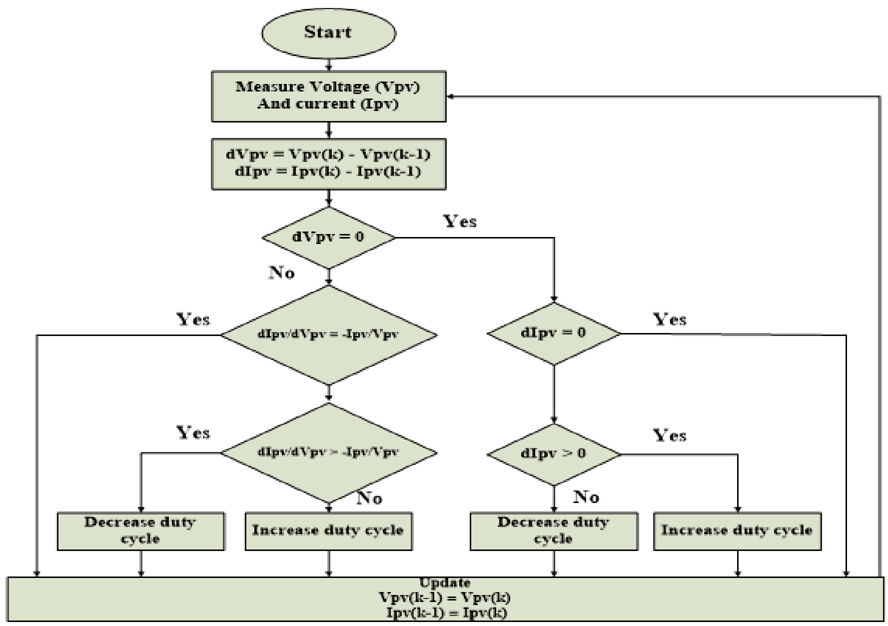

Figure 2 INC MPPT algorithm.

The actual photovoltaic voltage is matched with V_{dc}^* which is the output of the MPPT algorithm, as follows [31]

$$Vdc_e(m) = Vdc^*(m) - Vpv(m) \tag{17}$$

A PI controller then receives the error. A speed error is considered by the PI controller's output. $\omega_1^*(m)$ is written as

$\omega_1^*(m)$ is written as

$$\omega_1^*(m) = \omega_1^*(m-1) + K_{pd}\{V_{dce}(m) - V_{dce}(m-1)\} + K_{id}V_{dce}(m) \tag{18}$$

Where K_{pd} is proportionality and K_{id} is an integral constant.

This is the reference speed at the $\mathrm{M_{th}}$ sampling instant.

$\omega_2^*(m)$ is another speed reference produced by pump's affinity law that can be considered as a feed-forward component [32]

$$\omega_2^*(m) = [P_{pv}(m)/K_1]^{1/3} \tag{19}$$

Where K_1 is the proportionality constant

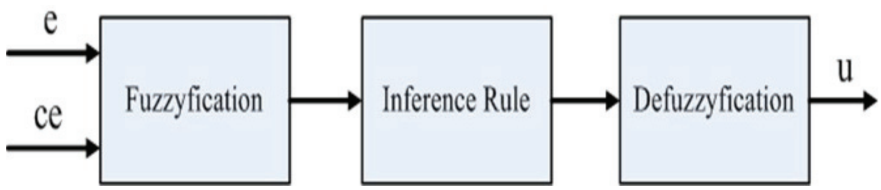

Figure 3 Structure of fuzzy logic control.

$\omega_2^*(m)$ is the highest-rated speed resembling the given irradiance. The system's dynamic response is very poor. Hence, the feed-forward component, which consists of photovoltaic power and the proportionality constant, supports rapid dynamic response by straightaway reflecting the photovoltaic power on speed [33].

ω^* is evaluated as

$$\omega^*(m) = \omega_1^*(m) + \omega_2^*(m) \tag{20}$$

The actual speed and the reference speed are compared; the resulting error is given below.

$$e(m) = \omega^*(m) - \omega_r(m) \tag{21}$$

Both error (e) and the rate of change error (ce) is fed to a controller, i.e., fuzzy logic controller.

4.2 Fuzzy Logic Control

This control has been utilized in various control and automation applications. The linguistic rules are used to regulate fuzzy logic [34]. Figure 3 depicts the control's structure. The structure has three blocks, i.e., fuzzification, inference fuzzy rule, and defuzzification.

4.2.1 Fuzzyfication

This converts crisp input and output variables to the linguistic variable (Fuzzy set). A triangular-shaped membership function is selected here because of its simplicity and best control performance results. The two variables i.e. output and input are adopted into seven membership functions as NB, NM, NS, ZE, PS, PM, PB, and nine membership functions for output The membership functions are normalized in the universe of discourse within -1 and 1 presented in Figure 4.

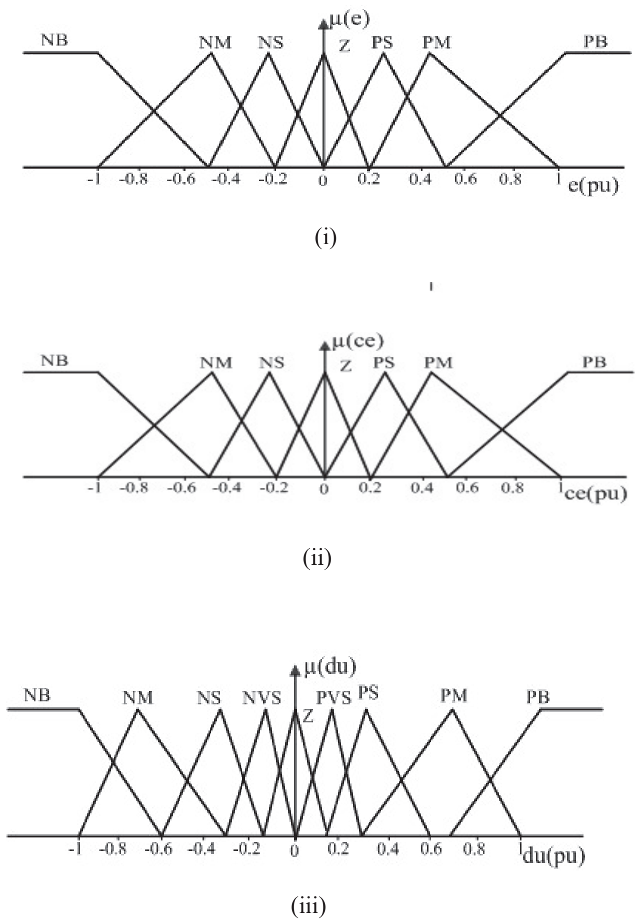

Figure 4 Membership Function of (i) e, (ii) ce, and (iii) output.

4.2.2 Inference fuzzy rules

In linguistic form, a bunch of rules are comprised in inference fuzzy rule represented as If-then rules created by the experience of specialist's knowledge [35]. Depending on the membership function, 49 rules are obtained here. The rules are presented in Table 1.

4.2.3 Defuzzfication

This converts the linguistic output variables produced by rules of FLC to crisp output. The crisp output is obtained using the centre of gravity defuzzification method.

Table 1 Fuzzy logic control rule

ce \ e	NB	NM	NS	ZE	PS	PM	PB
NB	NVB	NVB	NVB	NB	NM	NS	ZE
NM	NVB	NVB	NB	NM	NS	ZE	PS
NS	NVB	NB	NM	NS	ZE	PS	PM
ZE	NB	NM	NS	ZE	PS	PM	PVB
PS	NM	NS	ZE	PS	PM	PB	PVB
PM	NS	ZE	PS	PM	PB	PVB	PVB
PB	ZE	PS	PM	PB	PVB	PVB	PVB

4.3 Field Oriented Control

The speed is controlled by utilizing this control. The ω_e along with the rate of change of ω_e is sent to the fuzzy logic controller. The reference torque T_e^* is the output T_e^* is

$$T_e^*(m) = T_e(m-1) + K_p\{\omega_e(m) - \omega_e(m-1)\} + K_i\omega_e(m) \tag{22}$$

The *q* axis current i_{qs}^* is derived from T_e^* as follows

$$I_{qs}^* = KT_e^* \tag{23}$$

As the motor is required to be driven below rated speed for water pumping, field wakening is not needed. As a result, the current I_d^* on the *d* axis is held at zero.

By utilizing inverse Park's transform, both *d* and *q* axis currents produce reference current (i_a^*, i_b^*, i_c^*). A hysteresis controller is utilized to generate pulses for VSI by comparing the actual stator currents with reference stator currents

5 Results and Discussion

The system proposed in this article is simulated in MATLAB/Simulink and evaluated under various operational conditions. The simulation is verified and tested in real-time on an OPAL-RT platform.

5.1 Starting and Steady-state Performance

The photovoltaic parameters shown in Figure 5 has a fine tracking of MPP and reaches its steady-state value of 300 V, 4.3 A and 1261 W at 1000 w/m^2

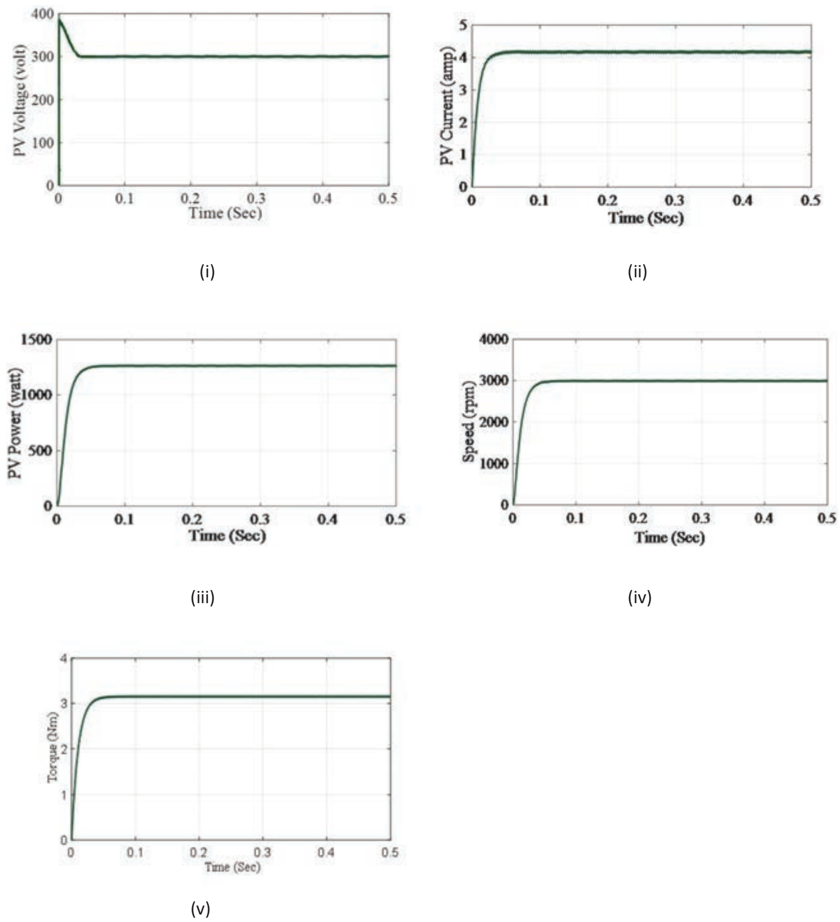

Figure 5 Reponses of (i) PV voltage (ii) PV current (iii) PV power (iv) Motor speed (v) Motor torque, for 1000 W/m^2 insolation under steady-state.

within a fraction of a second shown Figure 5(i),(ii), and (iii). The motor parameters attain their rated values respectively, as can be seen in Figure 5(iv) and 5(v).

5.2 Dynamic State Performance

To substantiate the suitable performance of the system under variable climatic states, the irradiance is reduced from 1000 to 400 W/m^2 and then returned to 1000 W/m^2 while keeping the temperature constant as shown in Figure 6. As

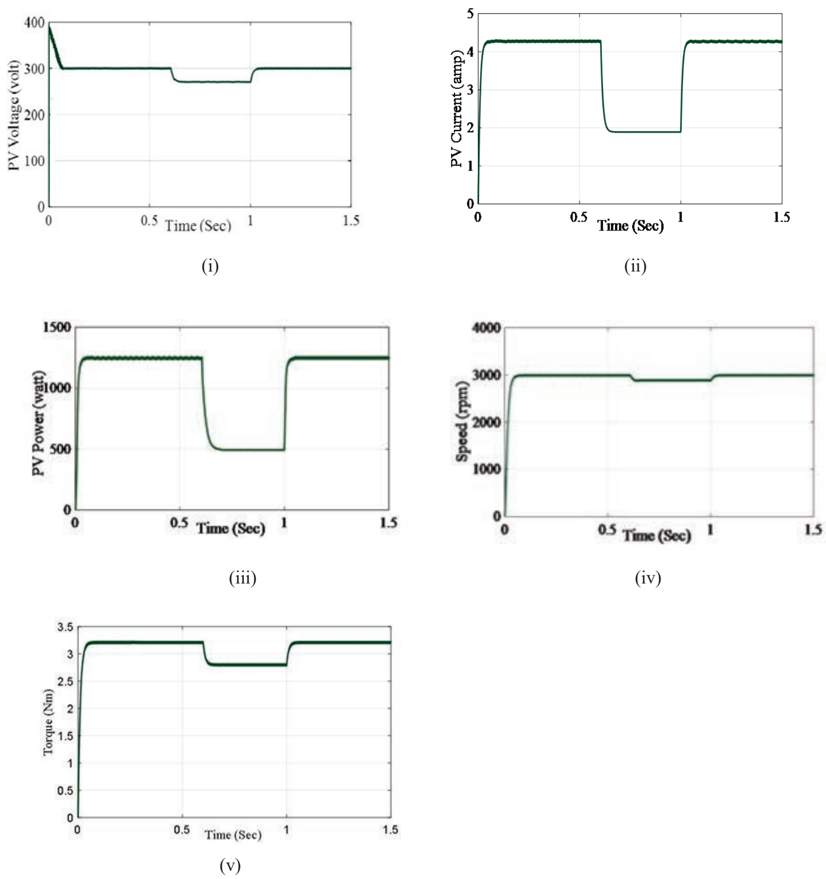

Figure 6 Reponses of (i) PV voltage (ii) PV current (iii) PV power (iv) Motor speed (v) Motor torque, for 1000 W/m^2 insolation under dynamic-state.

a result, the PV voltage does not change significantly as a result of MPPT operation, as shown in Figure 6(i). However, as illustrated in Figure 6(ii) and 6(iii), the current as well as power are reduced by nearly half because they are directly proportional to irradiance. The motor parameters, i.e., speed and torque, are also varied accordingly during the variation of the solar irradiance, illustrated in Figure 6(iv) and 6(v). At lower irradiance, peak power extracted is less, therefore there is a reduction in ω_r and T_e. Hence, the water flow from the pump is reduced.

5.3 Performance Under Partial Shading Condition

Under these conditions, there is a reduction in the PV voltage of series-connected PV modules of a photovoltaic array. Hence, the total power is also reduced. However, the speed remains at a specified value due to the control action of the closed-loop fuzzy logic controller demonstrated in Figure 7. To verify the same, four out of twenty modules of the PV array are removed to mimic the effect of partial shading. Under such conditions, both photovoltaic array and motor responses are presented in Figure 7(i) to 7(iv). Due to the

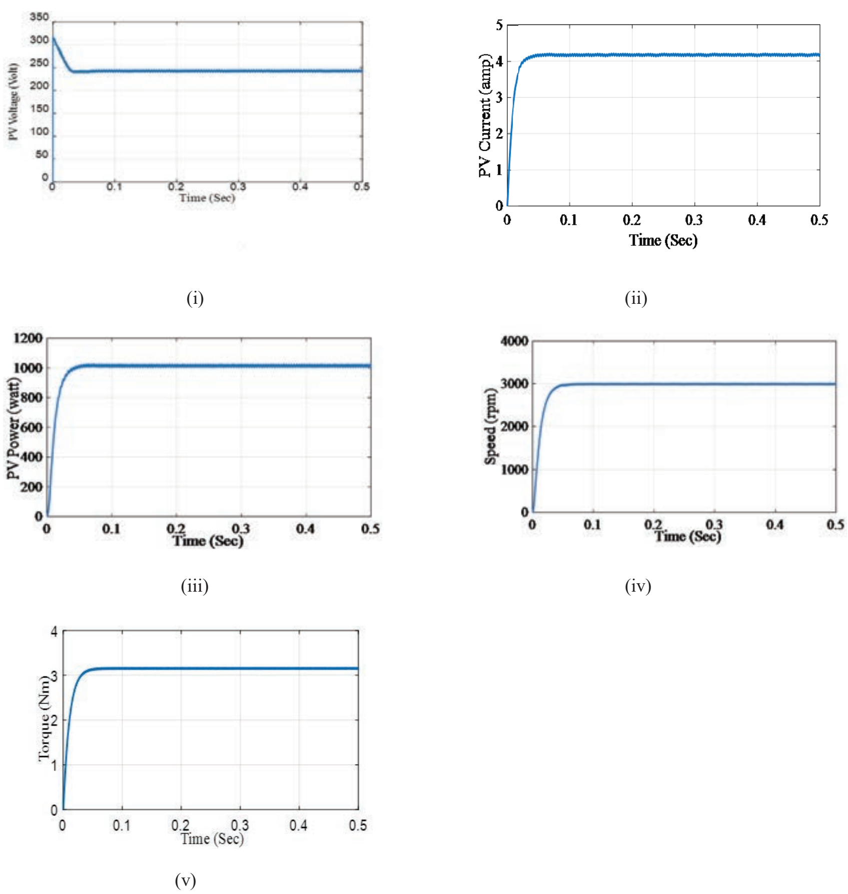

Figure 7 Responses of (i) PV voltage (ii) PV current (iii) PV power (iv) Motor speed (v) Motor torque, for 1000 W/m^2 insolation under partial shading condition.

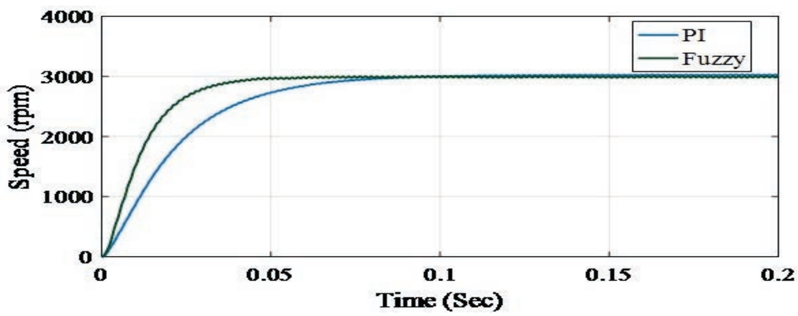

Figure 8 Speed response of PI and Fuzzy logic controller.

robust controller, the BLDC motor pump adequately supplies the full capacity of water even in the condition of partial shading.

Figure 8 shows the comparison of motor speed response by implementing both PI and fuzzy logic controllers. The rising time of speed response in the case of the PI controller is 4.8 ms whereas in the case of the fuzzy logic controller it is 2.5 ms. The speed response by using PI controller settled down to steady state at 7.6 ms, however by using fuzzy logic controller it settled down to steady state at 4 ms. Hence When compared to the traditional PI controller, the fuzzy logic controller provides a faster speed response.

6 Real-Time Implementation with OPAL-RT

The OPAL-RT environment validates the MATLAB simulation responses in real-time.

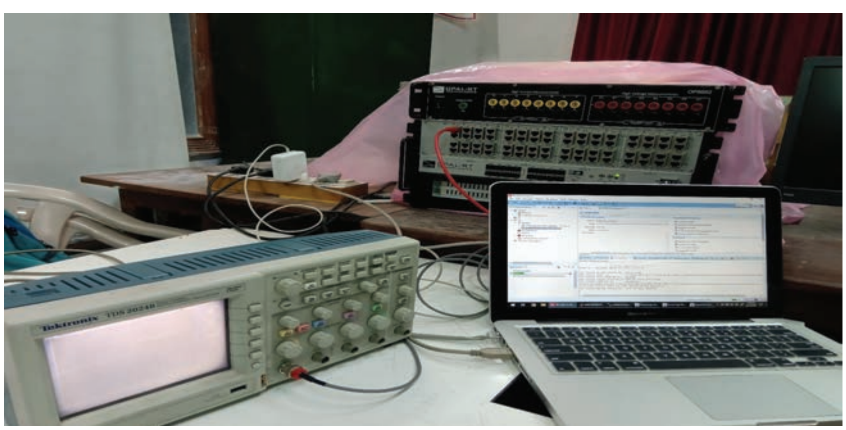

Figure 9 OPAL-RT interfaced with console PC.

6.1 Starting and Steady-state Performance

The waveforms shown in Figure 10 depict the performance results of the photovoltaic array and motor pump respectively. The various system parameters are recorded under this condition. The motor–pump and photovoltaic array reached the steady-state i.e., $Vpv = 300$ v $P_{pv} = 1.26$ W, $I_{pv} = 4.3$ A,

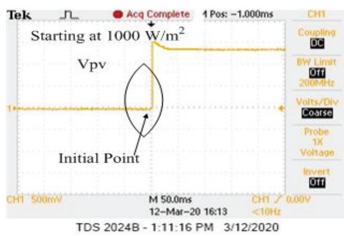

(i)

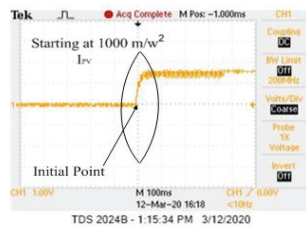

(ii)

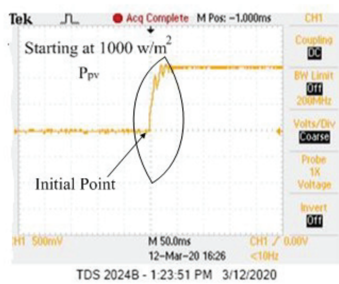

(iii)

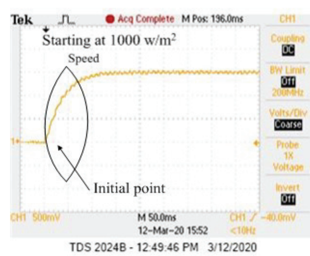

(iv)

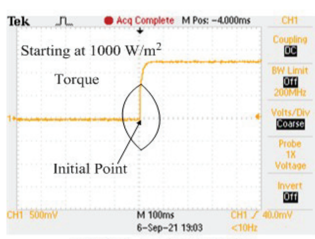

(v)

Figure 10 Real time responses with OPAL-RT (i) PV voltage (ii) PV current (iii) PV power (iv) Motor speed (v) Motor torque.

$N = 3000$ rpm, $T = 3.18$ Nm resembling to maximum power point as shown in Figure 10(i) to 10(iv).

6.2 Dynamic State Performance

The responses under this state are demonstrated in Figure 11. By decreasing the irradiance, the photovoltaic voltage has reduced slightly, but the current

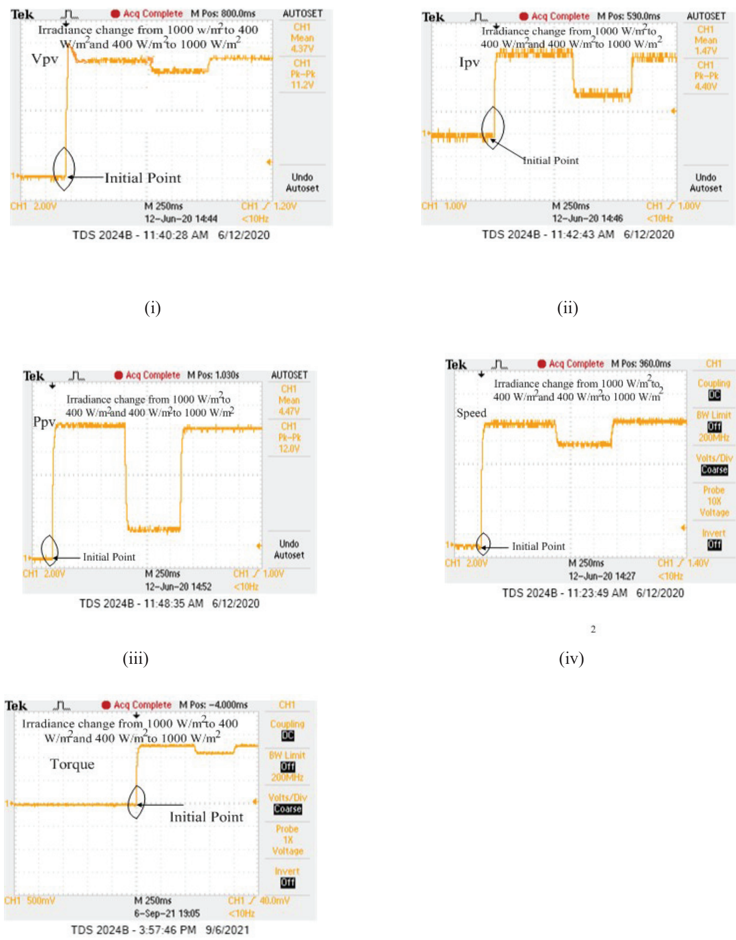

(v)

Figure 11 Real time responses with OPAL-RT (i) PV voltage (ii) PV current (iii) PV power (iv) Motor speed (v) Motor torque.

and hence power has decreased proportionally can be seen in Figure 11(i), (ii), and (iii). The parameters of the motor are also very consequently illustrated in Figure 11(iii) and 11(iv).

6.3 Performance Under Partial Shading Condition

The responses of the motor and photovoltaic array under these conditions are presented in Figure 12. This condition is realized by reducing four out

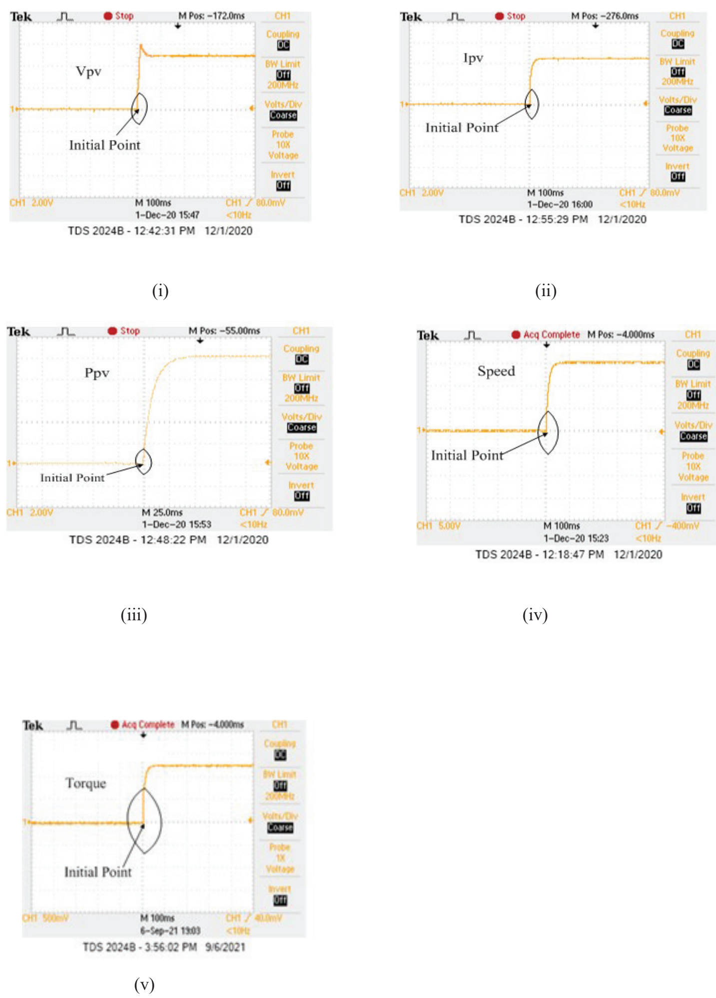

Figure 12 Real time responses with OPAL-RT (i) PV voltage (ii) PV current (iii) PV power (iv) Motor speed (v) Motor torque.

of twenty series-connected modules of a photovoltaic array. Both the voltage as well as the power of the photovoltaic array are reduced because of the partial shading illustrated in Figure 12(i) and 12(iii). However, the speed remains the same due to the closed-loop fuzzy logic controller demonstrated in Figure 12(iv). Hence, the BLDC motor pump delivers water at full capacity even with partial shading.

7 Conclusion

A standalone single-stage photovoltaic array fed a 2-DoF controlled water pumping system is presented. The system is apprehended under both steady and dynamic state at standard testing conditions using MATLAB Simulink and validated using OPAL-RT simulator. The feedback loop, which includes fuzzy logic control, greatly enhance the efficiency of the compensated system. The system response has been further accelerated by incorporating the feed-forward term under dynamic conditions. The system offers a quick, fruitful solution for water pumping.

Appendix

Solar PV Parameter:

$$V_{oc} = 19.8\text{ V},\quad I_{sc} = 4.8\text{ A},\quad V_m = 15.44,\quad I_m = 4.3\text{ A}$$

BLDC Motor Parameter

$$\text{P} = 3000\text{ rpm},\quad R_s = 2.87\ \Omega,\quad L_s = 8.5\text{ mH},$$

$$\text{Rated DC link voltage} = 300\text{ V},\quad T_{rated} = 3.18\text{ Nm}$$

References

[1] Foster R, Ghassemi M, Cota. M. Renewable Energy and the Environment. CRC press; 2009.

[2] M. Kolhe, J.C. Joshi, D.P. Kothari. Performance analysis of a directly coupled photovoltaic water-pumping system *.IEEE Trans. on Energ Conv.* 9: 613–618.

[3] S. Shukla, B. Singh. Improved power quality converter for three-phase grid interfaced PV array fed reduced current sensor-based induction

motor drive for water pumping. *International Transaction on Electrical Energy System*, 2020.
[4] D. Weiner, A. Levinson. An optimal operation design of a photovoltaic DC motor coupled water pumping system. In India, 1990 Conf Proc. IEEE Ind. Appl. Society Annu. Meeting, USA.
[5] M. Kolhe, J.C. Joshi, D.P. Kothari. Performance analysis of a directly coupled photovoltaic water-pumping system. *IEEE Trans. Energy Convers.*, 2004, 19(3): 613–618.
[6] L. Davies, M. Malengret, Application of induction motor for solar water pumping. In Swaziland, 1992 Conf Proc. IEEE. 3D.
[7] B. Singh, S. Murshid, A grid-interactive permanent-magnet synchronous motor-driven solar water-pumping system. *IEEE Trans. Ind. Appl.*, 2018, 54(5): 5549–5561.
[8] P.K. Singh, B. Singh. Brushless DC motor drive with power factor regulation using Landsman converter. IET Power Electron, 2016, 9: 900–910.
[9] R. Singh, B Singh, BLDC motor driven water pump fed by solar photovoltaic array using boost converter. In India, 2015 Conf. Proc. IEEE India Conference (INDICON), 2015.
[10] B. Naidu Kommula, V. Reddy Kota. Direct instantaneous torque control of Brushless DC motor using firefly Algorithm based fractional order PID controller. *Journal of King Saud University – Engineering Sciences*. 2020, 32: 133–140.
[11] Y. Zhou, D. Zhang, X. Chen, and Q. Lin. Sensorless direct torque control for saliency permanent magnet brushless DC motors, *IEEE Trans. Energy Convers.,* 2016, 31(2): 446–454.
[12] S. Wang, A. C. Lee. A 12-step sensorless drive for brushless DC motors based on back-EMF Differences, *IEEE Trans. Energy Convers.*, 2015, 30(2): 646–654.
[13] V. Bist, B. Singh. A brushless DC motor drive with power factor correction using isolated zeta converter. *IEEE Trans. Ind. Info*, 2014, 10: 2064–2072.
[14] Md Z.Youssef. Design and performance of a cost-effective BLDC drive for water pumping application. *IEEE Trans.on Indus. Electron*, 2015, 62: 3277–3284.
[15] S. Lukas, An investigation of PV powered brushless DC motors for solar pumping: an autonomous and elegant integration of electric motor and pump for use with a solar domestic hot water system (VDM Verlag, Germany, 2008).

[16] R. Kumar, B. Singh. Simple brushless DC motor drive for solar photovoltaic array fed water pumping system. *IET Power Electron*. 2016, 9: 1487–1495.

[17] R. Kumar and B. Singh. Single Stage Solar PV Fed Brushless DC Motor Driven Water Pump. *IEEE Journal of Emerging and Selected Topics in Power Electronics*, 2017, 9(3): 1377–1385.

[18] M. Nasir Udin, Tawfik S. Radwan, M. Azizur Rahman. Performance of Fuzzy-Logic-Based Indirect vector control for induction motor drive. *IEEE Transaction on Industry Applications*, 2002, 38(5).

[19] D.K. Panicker, Ms. Remya Mol. Hybrid PI-Fuzzy Controller for Brushless DC motor speed control. *J. of Electr and Electron Eng.,* 2013, 8: 33–43.

[20] J. Ahmed, Z. Salam. An improved perturb and observe (P&O) maximum power point tracking (MPPT) algorithm for higher efficiency. *Appl. Energy*, 97–108.

[21] K. Rahrah, D. Rekioua, T. Rekioua. Photovoltaic pumping system in Bejaia climate with battery storage. *Int. J. Hydr. Energ,* 2015, 40: 13665–13675.

[22] M.A. Elgendy, B Zahawi, D.J. Atkinson. Comparison of directly connected and constant voltage controlled photovoltaic pumping systems, *IEEE Trans. Sustain. Energ.*, 2010, 1: 184–192.

[23] S. Djeriou, A. Kheldoun, A. Mellit. Efficiency Improvement in Induction Motor-Driven Solar Water Pumping System Using Golden Section Search Algorithm. *Arab. J. Sci. Eng.*, 2018, 43: 3199–3211.

[24] M. Dubey, S. Sharma, R. Saxena, Solar power driven position sensor less control of permanent magnet brushless DC motor for refrigerator point. *Int Trans on Electr Energ Syst.*, 2020, 30.

[25] R. Kumar, B. Singh. Single Stage Solar PV Fed Brushless DC Motor Driven Water Pump. *IEEE Jourmal of Emerging and Selected Topics in Power Electron.*, 2017, 5: 1377–1385.

[26] D. Verma, S. Nema, A.M. Shandilya, S.K. Dash.Maximum power point tracking (MPPT) techniques: Recapitulation in solar photovoltaic systems, *Renew. Sustain. Energy Rev.*, 2016, 54: 1018–1034.

[27] T. Esram, P.L. Chapman. Comparison of photovoltaic array maximum power point tracking techniques, *IEEE Trans. Energy Convers*, 2007, 22(2): 439–449, Jun. 2007.

[28] A. Garrigos, J.M. Blanes, J.A. Carrascoa, J.B. Ejea. Real time estimation of photovoltaic modules characteristics and its application to maximum power point operation. *Renew. Energy*, 2007, 32: 1059–1076.

[29] M. Calavia, J.M. Perie, J.F. Sanz, J. Sallan. Comparison of MPPT strategies for solar modules. In Spain, 2014 International conference on Renewable Energies Power Quality (ICREPQ), 1440–1445.

[30] B. Subudhi, R. Pradhan. A Comparative Study on Maximum Power Point Tracking Techniques for Photovoltaic Power Systems, *IEEE Trans on Sustainable Energ*., 2013, 4: 89–98.

[31] S. Murshid, B. Singh. Implementation of PMSM Drive for a Solar Water pumping System. *IEEE Trans. on Ind. Appl.*, 2019, 55: 4956–4964.

[32] W.V. Jones. Motor Selection Made Easy: Choosing the Right Motor for Centrifugal Pump Applications. *IEEE Indus Appl Mag.*, 2013, 19: 36–45.

[33] S. Shukla, B. Singh. Single-Stage PV Array Fed Speed Sensorless Vector Control of Induction Motor Drive for Water Pumping, *IEEE Trans. on Ind. Appl*., 2018, 54: 3575–3585.

[34] Tony Mathew, Sam Caroline Ann, Closed Loop Control of BLDC Motor Using a fuzzy logic controller. In India 2013 International Conf. on Advanced Computing and Communication Systems (ICACCS), 2013.

[35] E. Essam, A. Zahab, Aziza M. Zaki, M. Mohamed, E.I. Sotouhy. Design and control of a standalone PV water pumping system. *J. of Electr. Syst. and Info. Tech*., 2017, 4: 322–337.

Biographies

Biranchi Narayan Kar received his BE in Electrical Engineering from Seemanta Engineering College, Jharpokharia, Odisha, India in 2005 and M.Tech in Power Electronics and Drives from National Institute of Technology Rourkela, Odisha, India in 2011. He is currently working toward his PhD in the Electrical Engineering at Motilal Nehru National Institute of Technology, Allahbad, Pryagraj, Utter Pradesh, India His research interests include power electronics Drives and Renewable Energy.

Paulson Samuel received the Bachelor of Engineering (Electrical) degree from the G. S. Institute of Technology and Science, Indore, India, in 1984, and the Master of Engineering in Computer Science and Engineering degree from Motilal Nehru National Institute of Technology, Allahabad, India, in 1998. He completed Ph.D in electrical engineering from Motilal Nehru National Institute of Technology, Allahabad, India, in 2013. From 1990 onward, he has been a faculty member in the Department of Electrical Engineering, Motilal Nehru National Institute of Technology, where he is presently a Professor. From 1984 to 1990, he was an Engineer at the National Thermal Power Corporation, New Delhi, India. His research interests include power quality, distributed generation, automation, control of power converters, and multilevel inverters.

Jatin Kumar Pradhan received his BE in Electrical Engineering VSSUT,burla, Odisha in 2008, MTech in Power Electronics and Drives from National Institute of Technology Rourkela, Odisha, India in 2011 and PhD from IIT Bhubaneswar, Odisha, India in 2019. He is currently working as Assistant Professor in the Electrical Engineering Dept. at VSSUT, Burla, Odisha, India. His research interests include Control of MIMO System, Robust Control, Control System Applications.

Amit Mallick received his B.Tech in Electrical Engineering from NM Institute of Engineering and Technology, Bhubaneswar Odisha, India in 2013 and M.Tech in Power System from VSSUT, Burla, Odisha, India in 2011. He is currently working as Assistant Professor in the Electrical Engineering Dept. at VSSUT, Burla, Odisha. His research interests include Power electronics, Power system and Microgrid operation and protection.